

SUPPLEMENTARY INFORMATION

Composite CdS/TiO₂ powders in the selective reduction of 4-nitrobenzaldehyde by visible light: relation between preparation, morphology and photocatalytic activity

M. Milani¹, M. Mazzanti¹, S. Caramori¹, G. Di Carmine¹, G. Magnacca², A. Molinari^{1*}

¹ Dipartimento di Scienze Chimiche, Farmaceutiche ed Agrarie, Università di Ferrara, Via L. Borsari 46, 44121 Ferrara, Italy

² Dipartimento di Chimica, Università di Torino, Via P. Giuria 7, 10125 Torino, Italy

Table of Contents

Figure S1. A) Adsorption/desorption isotherms of CdS/TiO₂ samples; B) Pore size distribution curves; C) Pore area distribution curves. The logarithmic scale, where used, allows evidencing better the large pore region. The broken lines indicate the threshold between micro and meso/macropores.

Figure S2. Single photon time emission decay of powder CdS/TiO₂-1

Figure S3. Single photon time emission decay of powder CdS/TiO₂-2

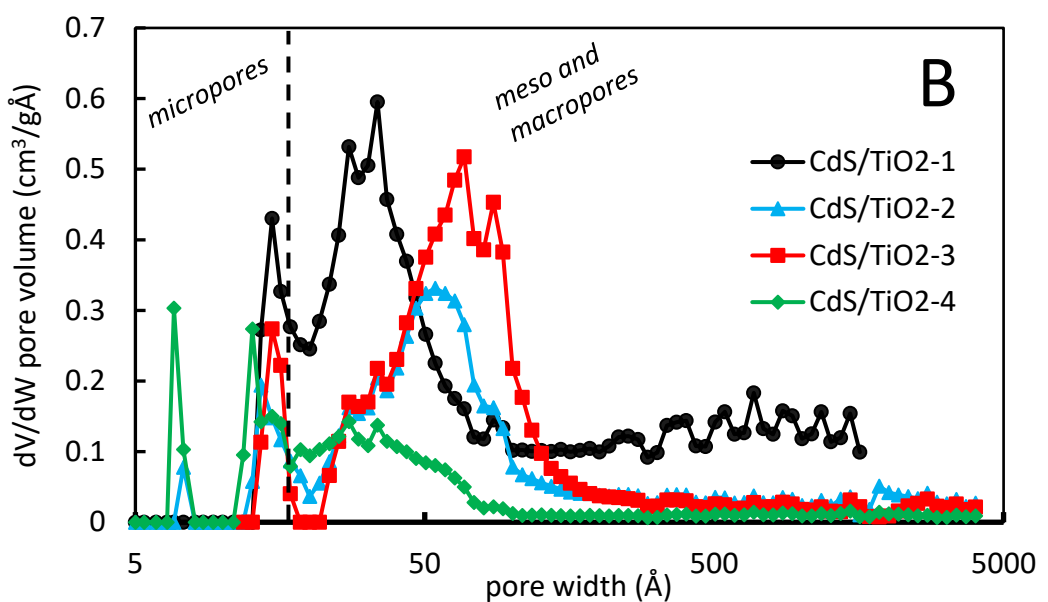
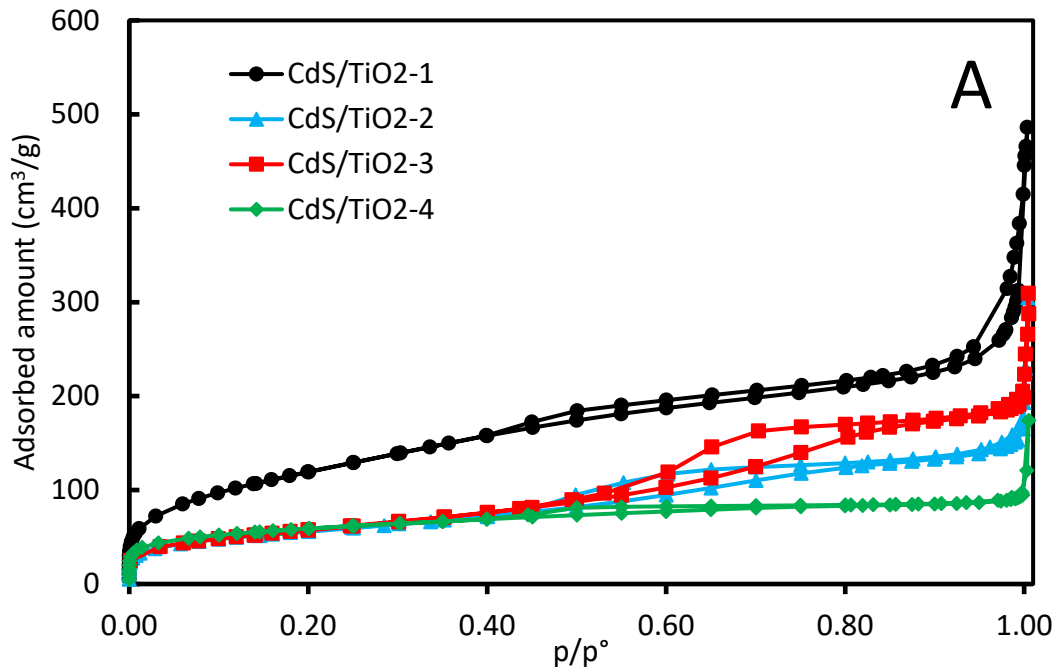
Figure S4. Energy band gap of CdS/TiO₂ – 1/4 obtained using the baseline method (Ref. 33) coupled with that described by Tauc: for TiO₂ the fundamental fit is applied using the relation $(Fhv)^{\alpha} = A \times (hv - Eg)$, where F is the Kubelka-Munk coefficient, $\alpha=1/2$ for an indirect band gap, A is a proportionality constant and hv is the photon energy; additionally, a linear fit used as an abscissa is applied for the slope below the fundamental absorption. An intersection of the two fitting lines gives the band energy estimation (red).

Table S1. Band gap values obtained from Figure S4.

Figure S5. Spectral changes obtained upon visible irradiation of deaerated suspensions of CdS/TiO₂ – 2 (3 g/L) in CH₃CN/2-PrOH (4/1, 3mL) mixture containing NBA (1×10^{-4} M).

Figure S6. Decrease of NBA concentration as a function of irradiation time for CdS/TiO₂ – 2 (squares), CdS (circles) and TiO₂ (triangles). The experimental conditions are the same of Figure 5. Values of CdS/TiO₂ – 2 (already present in Figure 5) are reported here for an easy comparison.

Figure S7. Kinetic rates calculation



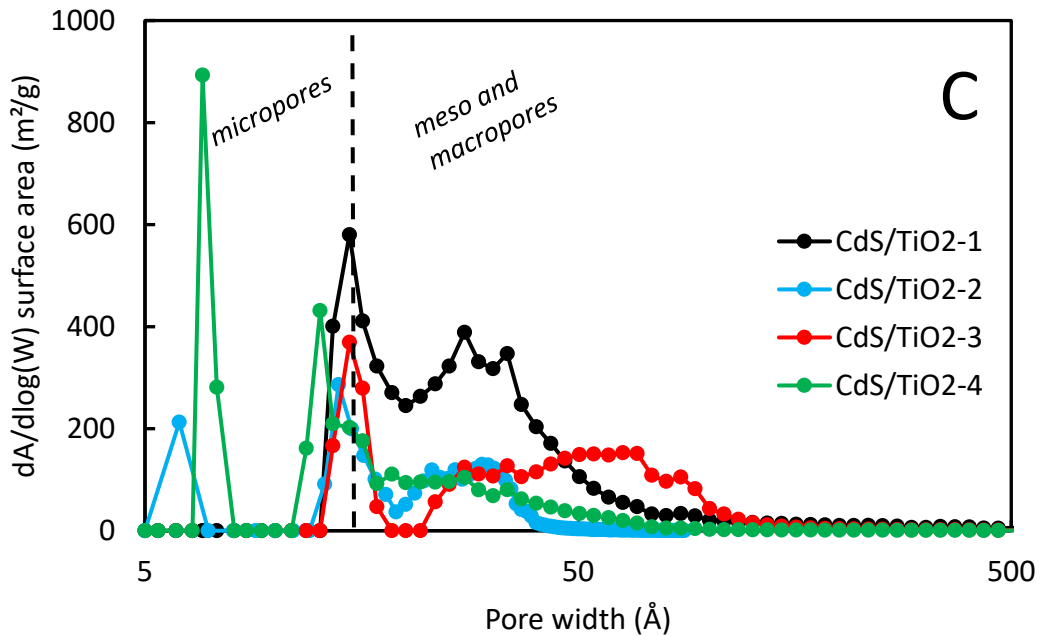
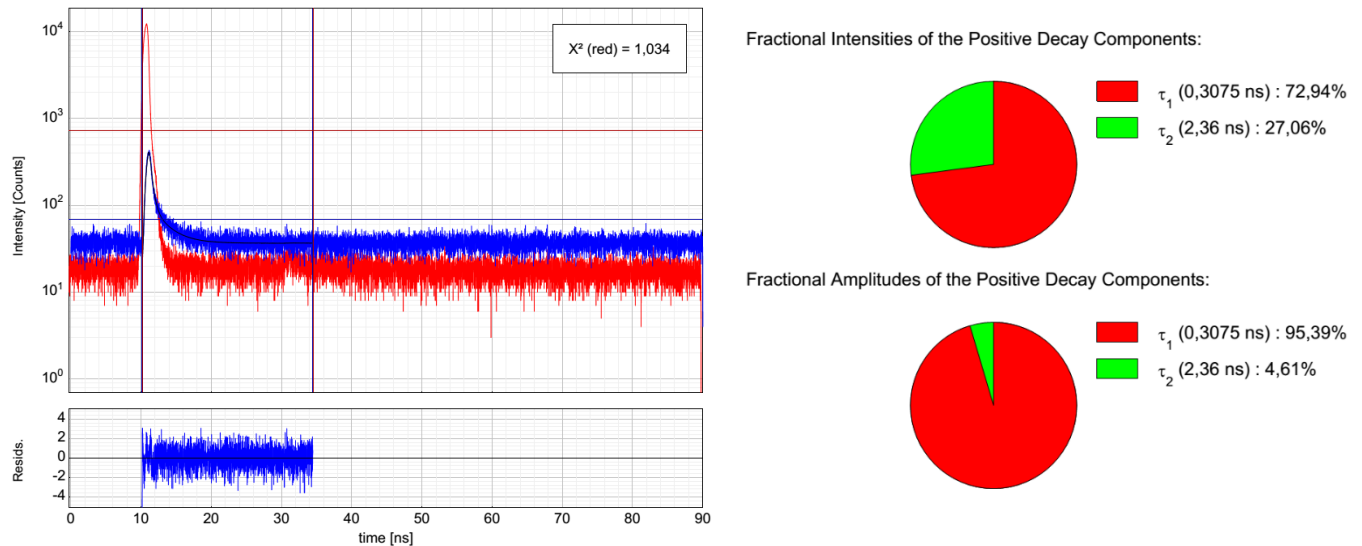
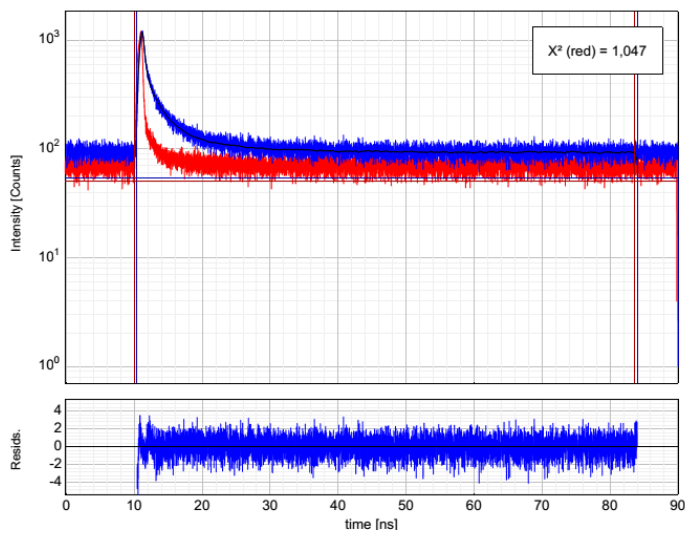


Figure S1

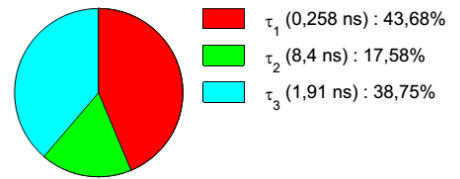


Parameter	Value	Conf. Lower	Conf. Upper	Conf. Estimation
A_1 [Cnts]	1740	-44	+44	Fitting
τ_1 [ns]	0,3075	-0,0082	+0,0082	Fitting
A_2 [Cnts]	84,2	-7,5	+7,5	Fitting
τ_2 [ns]	2,36	-0,23	+0,23	Fitting
Bkgr. Dec [Cnts]	68,6	-1,1	+1,1	Fitting
Bkgr. IRF [Cnts]	731	-24	+24	Fitting
Shift IRF [ns]	-0,25854	-0,00091	+0,00091	Fitting
A_{Scat} [Cnts]	-53400	-2700	+2700	Fitting

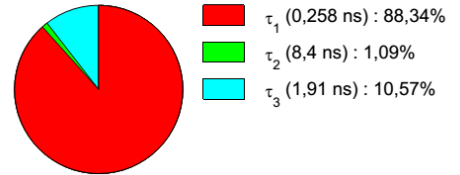
Figure S2



Fractional Intensities of the Positive Decay Components:



Fractional Amplitudes of the Positive Decay Components:



Parameter	Value	Conf. Lower	Conf. Upper	Conf. Estimation
A_1 [Cnts]	26600	-1300	+1300	Fitting
τ_1 [ns]	0,258	-0,013	+0,013	Fitting
A_2 [Cnts]	329	-46	+46	Fitting
τ_2 [ns]	8,4	-1,2	+1,2	Fitting
A_3 [Cnts]	3190	-190	+190	Fitting
τ_3 [ns]	1,91	-0,11	+0,11	Fitting
Bkgr. Dec [Cnts]	54,3	-1,7	+1,7	Fitting
Bkgr. IRF [Cnts]	50,93	-0,81	+0,81	Fitting
Shift IRF [ns]	-0,190	-0,015	+0,015	Fitting
A_{Scat} [Cnts]	-66000	-73000	+73000	Fitting

Figure S3.

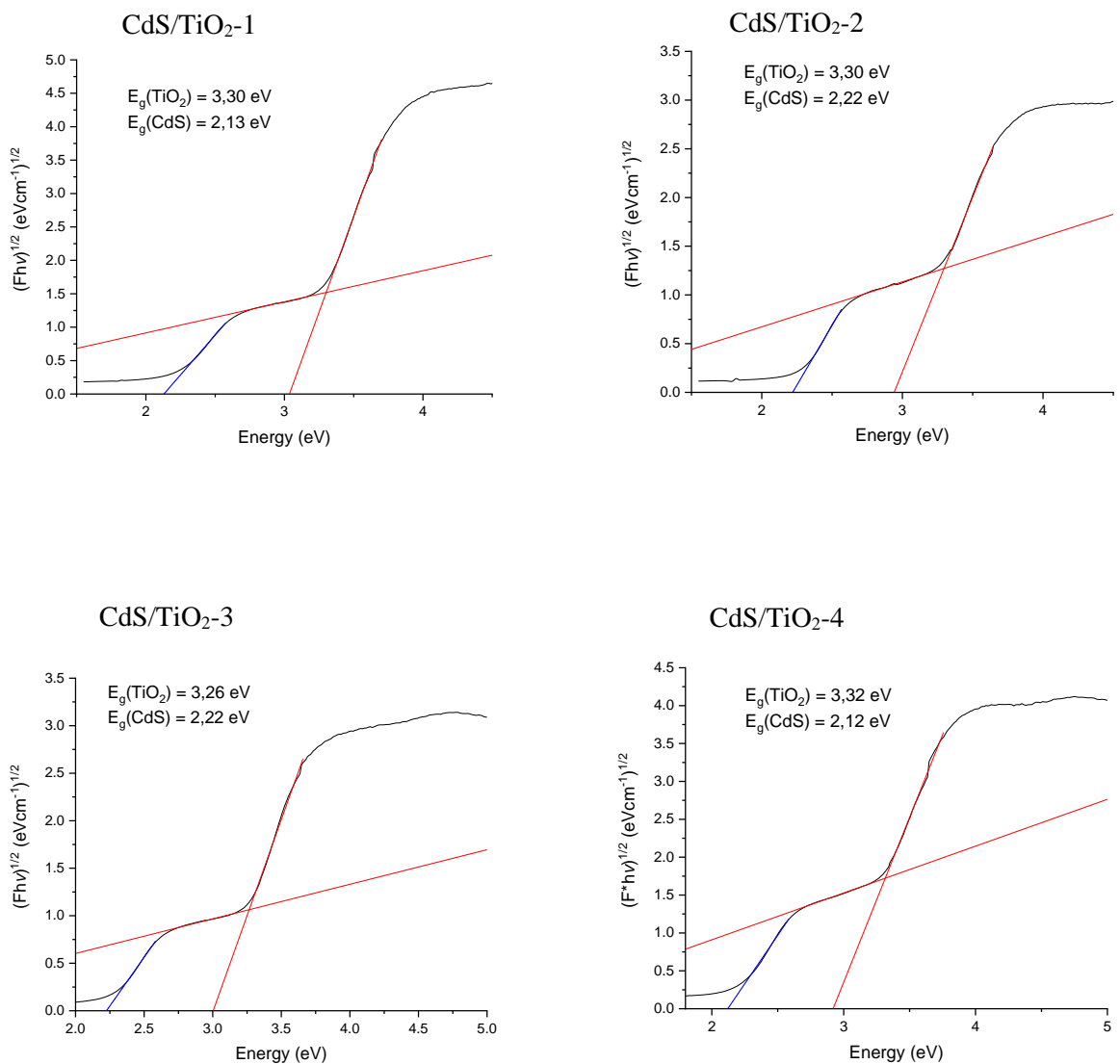


Figure S4.

Table S1. Band gap values obtained from Figure S4

Sample	CdS (eV)	TiO ₂ (eV)
CdS/TiO ₂ – 1	2.13	3.30
CdS/TiO ₂ – 2	2.22	3.30
CdS/TiO ₂ – 3	2.22	3.26
CdS/TiO ₂ – 4	2.12	3.32

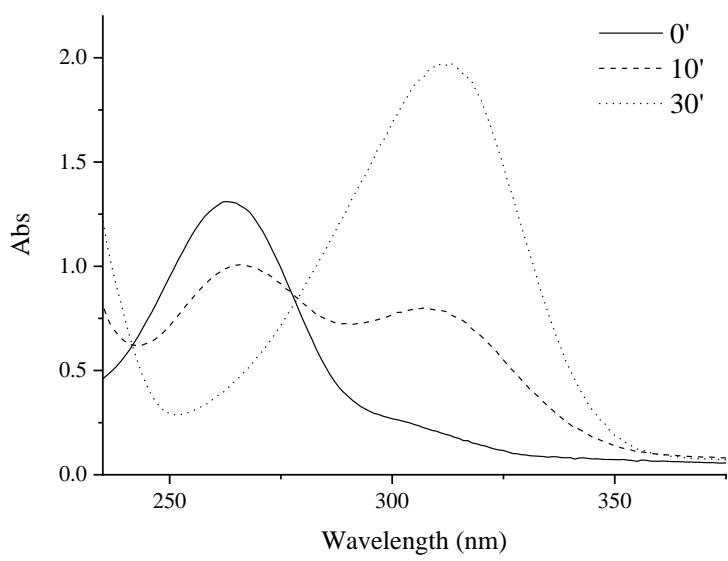


Figure S5.

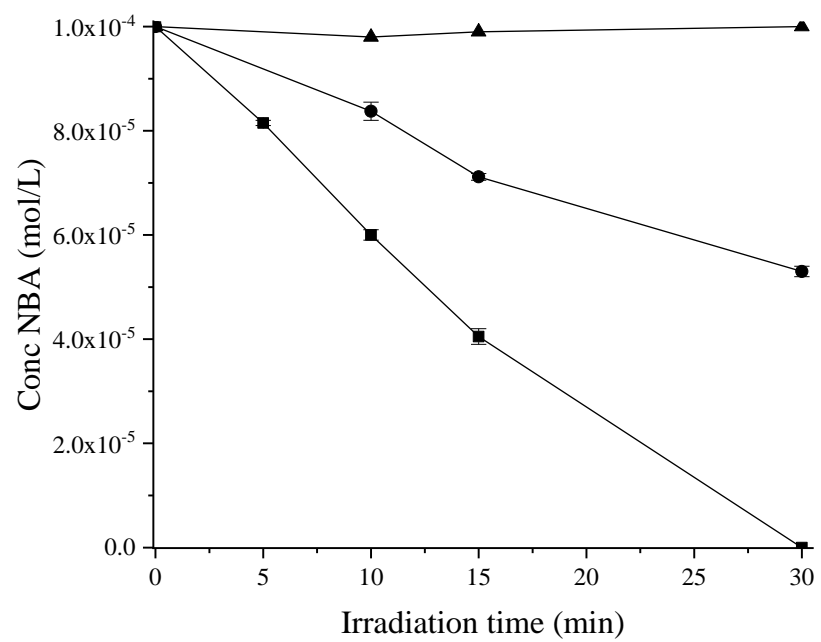


Figure S6

CdS/TiO₂-2

[NBA] _t	([NBA] ₀ -[NBA] _t)	-(t ₀ -t)	<i>v</i>
1,0E-04	0	0	0
8,0E-05	1,9E-05	5	3,9E-06
5,9E-05	4,1E-05	10	4,1E-06
4,0E-05	5,9E-05	15	3,9E-06
1,0E-06	9,9E-05	30	3,3E-06

CdS/TiO₂-3

[NBA] _t	([NBA] ₀ -[NBA] _t)	-(t ₀ -t)	<i>v</i>
1,0E-04	0	0	0
9,3E-05	6,1E-06	5	1,2E-06
7,3E-05	2,7E-05	10	2,7E-06
5,3E-05	4,7E-05	15	3,1E-06
8,2E-06	9,2E-05	30	3,0E-06

CdS/TiO₂-4

[NBA] _t	([NBA] ₀ -[NBA] _t)	-(t ₀ -t)	<i>v</i>
1,0E-04	0	0	0
8,0E-05	1,9E-05	15	1,3E-06
5,0E-05	5,0E-05	30	1,7E-06
2,4E-05	7,5E-05	45	1,7E-06
0	1,0E-04	60	1,7E-06

CdS/TiO₂-1

[NBA] _t	([NBA] ₀ -[NBA] _t)	-(t ₀ -t)	<i>v</i>
1,0E-04	0	0	0
8,0E-05	2,0E-05	30	6,7E-07
2,2E-05	7,7E-05	60	1,3E-06
6,7E-06	9,3E-05	120	7,8E-07
5,2E-07	9,9E-05	150	6,6E-07

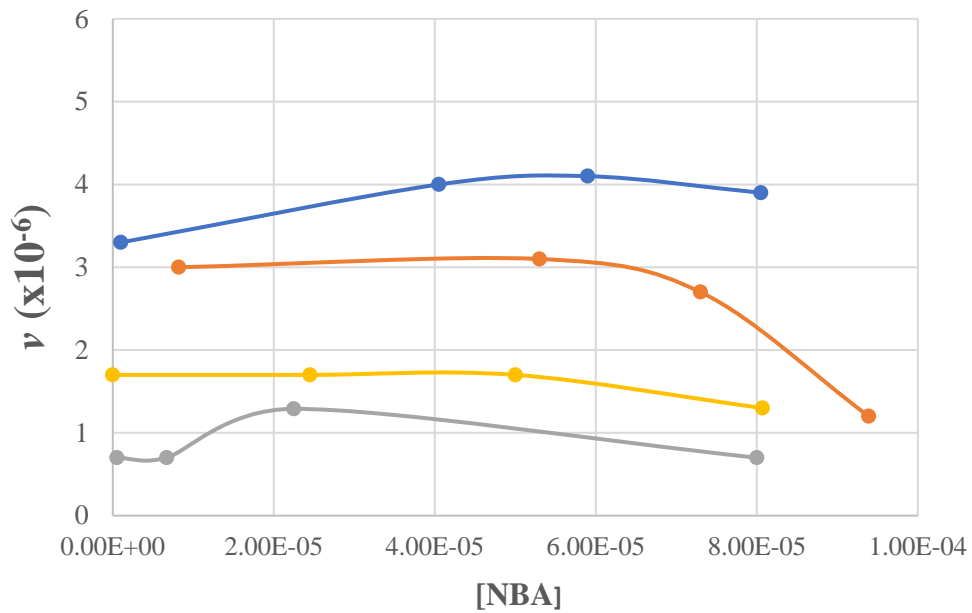


Figure S7.